



Cholesterol modulates the liposome membrane fluidity and permeability for a hydrophilic molecule



Samar Kaddah^{a,b}, Nathalie Khreich^a, Fouad Kaddah^c, Catherine Charcosset^b,
Hélène Greige-Gerges^{a,*}

^a Bioactive Molecules Research Laboratory, Faculty of Sciences, Lebanese University, Lebanon

^b Laboratoire D'Automatique et de Génie des Procédés (LAGEP), Université Claude Bernard, Lyon 1, France

^c École Supérieure D'ingénieurs de Beyrouth, Université Saint Joseph, Beyrouth, Mar Roukoz-Dekwaneh, Lebanon

ARTICLE INFO

Keywords:

Cholesterol
Fluidity
Liposomes
Mathematical models
Permeability
Release

ABSTRACT

The effect of cholesterol (CHOL) content on the permeability and fluidity of dipalmitoylphosphatidylcholine (DPPC) liposome membrane was investigated. Liposomes encapsulating sulforhodamine B (SRB), a fluorescent dye, were prepared by reverse phase evaporation technique (REV) at various DPPC:CHOL molar ratios (from 100:0 to 100:100). The release kinetics of SRB was studied during 48 h in buffer (pH 7.4) containing NaCl at 37 °C. The DPPC:CHOL formulations were also characterized for their size, polydispersity index and morphology. Increasing CHOL concentration induced an increase in the mean liposomes size accompanying with a shape transition from irregular to nanosized, regular and spherical vesicles. The release kinetics of SRB showed a biphasic pattern; the release data was then analyzed using different mathematical models. On the overall, the SRB release was governed by a non-Fickian diffusion during the first period (0–10 h) while it followed a Fickian diffusion between 10 and 48 h. Changes in DPPC liposome membrane fluidity of various batches (CHOL% 0, 10, 20, 30 and 100) were monitored by using 5- and 16 doxyl stearic acids (DSA) as spin labels. CHOL induced a decrease in the bilayer fluidity. Concisely, CHOL represents a critical component in modulating the release of hydrophilic molecules from lipid vesicles.

1. Introduction

Efficient delivery of drugs to living cells is a major challenge (Yang et al., 2016). Liposomes, spherical capsules composed of one or more bilayers enclosing an aqueous core, are the most common and well-investigated nanocarriers (Patil and Jadhav, 2015). They have been exhaustively studied for targeted drug delivery (Sercombe et al., 2015) and controlled release of drugs (Akbarzadeh et al., 2013). They represent simplified models of biological membranes mainly consisting of binary or ternary mixtures of lipids (Bretscher, 1973; Eeman and Deleu, 2010). Several liposomal formulations such as Doxil[®], Epaxal[®], DepoDur[™], Ambisome[®], etc., were marketed for several years (Bulbake et al., 2017). Liposomes are mainly prepared from amphiphilic lipid molecules such as phospholipids and sterols (Wu et al., 2015).

Dipalmitoylphosphatidylcholine (DPPC) is a major phospholipid in mammalian membranes which shows a thermotropic transition of 41 °C near the physiological temperature (Gmajner and Ulrih, 2011). Cholesterol (CHOL) is also a key component of eukaryotic cell biological membranes (Magarkar et al., 2014). Its effect on the structural and

dynamic properties of synthetic and natural membranes is well established. CHOL modulates the rigidity (Gracià et al., 2010; Najafinobar et al., 2016), thickness (Simons and Sampaio, 2011), stability (Miao et al., 2015) and fluidity of membranes (Peetla et al., 2013; Redondo-Morata et al., 2012; Takechi-Haraya et al., 2016). Moreover, CHOL content in membranes affects drug encapsulation efficiency (Haeri et al., 2014; Tabandeh and Mortazavi, 2013). It's worthwhile to note that the ratio between CHOL and phospholipid used in liposomes formulation to provide a controlled drug release is not well clarified (Briuglia et al., 2015; Miao et al., 2015). Therefore, it would be valuable to define the best combination of lipids and CHOL that allows a required controlled release of an encapsulated molecule (Fugit and Anderson, 2014).

To our knowledge, this study is the first to investigate the effect of cholesterol content on the permeability of DPPC bilayer for an encapsulated hydrophilic molecule, sulforhodamine B (SRB). Eleven batches of large unilamellar vesicles (LUVs) differing by DPPC:CHOL ratio (100:0, 100:2.5, 100:5, 100:10, 100:15, 100:20, 100:25, 100:30, 100:50, 100:75 and 100:100) are prepared by reverse phase

* Corresponding author.

E-mail addresses: hgreige@ul.edu.lb, greigeorges@yahoo.com (H. Greige-Gerges).

evaporation technique (REV). The different liposomal suspensions encapsulating a fluorescent dye, sulforhodamine SRB, are compared for the leakage of the fluorophore through the lipid bilayer at 37 °C over 48 h. The effect of CHOL content on the apparent release constants was analyzed by comparison of the SRB release kinetics data to several mathematical models: zero-order, first-order, Higuchi, Korsmeyer-Peppas, Hixson-Crowell, Weibull and Baker-Lonsdale models. Changes in DPPC liposome membrane fluidity with the CHOL content (10, 20, 30 and 100%) were investigated by electron paramagnetic resonance (EPR) spectroscopy using 5- and 16-doxyl stearic acid (DSA) as spins labels. Moreover, the liposome preparations were analyzed for their size, polydispersity index (PDI) and morphology by dynamic light scattering (DLS) and transmission electron microscopy (TEM), respectively. The results of this study could be used as a tool for assessing drug permeability, understanding and predicting the in vitro release of hydrophilic solutes from different liposome formulations thus leading to a better design of appropriate nanocarriers.

2. Materials and methods

2.1. Materials

Dipalmitoylphosphatidylcholine (DPPC) (purity ≥ 99%) is purchased from Lipoid GmbH, Germany. CHOL (purity 99%), SRB (95% content dye), gel sephadex G25 are all purchased from Sigma-Aldrich, Germany. 5- and 16-DSA are purchased from Sigma-Aldrich (St. Louis, MO, USA). Triton X-100 and Trizma Base are purchased from Sigma-Aldrich, Switzerland. The organic solvents chloroform and methanol are from Sigma-Aldrich, France and diethyl-ether is from VWR Chemicals ProLabo, France.

2.2. Preparation of large unilamellar vesicles containing SRB

Large unilamellar vesicles (LUVs) were prepared by reverse phase evaporation technique. of DPPC (25 μmol) was dissolved in 5 ml of a mixture of organic solvents: chloroform, diethyl-ether and methanol (6:6:1, v:v:v) (Khreich et al., 2008). The liposomal suspension was sonicated (Sonicator starsonic 35) for 1 min at 60 °C under nitrogen stream to avoid lipid oxidation. 0.75 ml of SRB solution (150 mM) prepared in 0.1 M tris-HCl buffer (pH 7.4) was added to the mixture followed by a sonication of the solution for 6 min at 60 °C under nitrogen stream. The organic solvents were removed at 45 °C using a rotary vacuum evaporator (Heidolph, Germany). A dark purple lipid film was obtained and SRB solution (1.5 ml) was added followed by a sonication for 5 min at 60 °C under a nitrogen stream. SRB was added to ensure its loading upon reconstitution of liposomes during evaporation and/or sonication steps. The liposomal suspension was stored at 4 °C for further manipulation.

The same protocol was used for the preparation of LUVs batches containing cholesterol. A stock solution of cholesterol was prepared in chloroform (25 mg/ml) and aliquots were added to the DPPC mixture before the first sonication at molar ratios DPPC: CHOL of 100:2.5, 100:5, 100:10, 100:15, 100:20, 100:25, 100:30, 100:50, 100:75 and 100:100. Three batches were prepared for each formulation.

2.3. Preparation of spin-labeled liposomes

Following the above-described protocol, the following formulations were prepared at various DPPC:CHOL ratios (100:0, 100:10, 100:20, 100:30, 100:100) with the exception that the spin label (5- or 16-DSA) was added to the liposomal suspensions at a DPPC:probe molar ratio of 100:1 before the first sonication. Three batches were prepared for each spin-labeled DPPC:CHOL formulation.

2.4. Extrusion and purification of liposomes

The liposome suspensions (SRB- and spin-labeled liposomes) were incubated in a 60 °C water bath for 35 min and then extruded using an “Avanti” mini-extruder (Avanti Polar Lipids, Switzerland) five times through a 1 μm polycarbonate membrane followed by five times through a 0.4 μm membrane. The extruded spin-labeled vesicles were ultracentrifuged (Optima™ Ultracentrifuge, Beckman Coulter, USA) at 40,000 g for 1 h at 4 °C and the resulting pellets were then kept in a desiccator overnight to remove the residual solvent before EPR analysis. The extruded SRB-loaded liposomes were centrifuged at 15000 rpm for 1 h at 4 °C to eliminate the excess buffer and the obtained pellet was suspended in tris-HCl (0.1 M; pH 7.4) buffer containing NaCl (150 mM). The buffer is added to maintain the osmolarity of the medium and to preserve the structure of the prepared liposomes. The resulting LUVs encapsulating SRB were separated from unloaded molecules by molecular sieve chromatography using sephadex G25 column. They were stored at 4 °C until use for fluorescence measurements.

2.5. Liposome characterization

2.5.1. Morphological analysis

Liposomes were imaged by transmission electron microscopy (TEM) using a CM120 microscope (Philips, Eindhoven, Netherlands). 10 μl of the liposome suspension was placed on copper grids and negatively stained by a sodium silicotungstate solution (1%) for 30 s. The excess of solution was removed with a filter paper and the air-dried stained samples were used for imaging.

2.5.2. Size analysis

The mean particle size of liposomes was determined by dynamic light scattering (DLS) technique using a Malvern Zetasizer Nano-series (Malvern Instruments Ltd, France). Dispersion Technology Software (DTS) v.5.10 was used to calculate the width of the fitted Gaussian size distribution which is displayed as the polydispersity index (PDI). The dispersity values reflect the nanoparticle size distribution (Masarudin et al., 2015) and ranged from 0 (monodispersed) to 1 (polydispersed) (Zaske et al., 2013). Before each DLS scan, the sample was stabilized for 5 min for the equilibration and the size measurements were performed in triplicate with at least 10 runs at 25 °C. Data were expressed as the mean ± standard deviation.

2.6. Fluorescence spectroscopy measurements

2.6.1. Preparation of liposome suspensions for fluorescence measurements

To obtain absorbance values of 1, the suspensions of SRB-loaded liposomes were diluted in tris-HCl buffer (0.1 M; pH 7.4) containing NaCl (150 mM). Measurements were performed at 532 nm which was determined to be the maximal absorbance wavelength for loaded-SRB. The optical density measurements were determined using a spectrophotometer (Nicolet evolution 300 Thermoelectron, England). The diluted batches were used for fluorescence measurements.

2.6.2. Permeability study

Permeability study was carried out at 37 °C by monitoring the release of SRB from liposomal suspensions over 48 h. The high concentration of encapsulated SRB in liposomes led to self-quenching followed by an increase in the fluorescence signal due to the release of SRB. Fluorescence measurements were performed using a spectrofluorometer (Thermo Spectronic, Aminco Bowman Series 2, USA). The excitation and the emission wavelength were 535 nm and 590 nm respectively. The release of SRB from LUVs is calculated according to the formula:

$$\text{Release SRB (\%)} = \frac{F_t - F_0}{F_{\text{max}}} \times 100 \quad (1)$$

where F_t is the fluorescence of the suspension at time t , F_0 is the initial fluorescence measured at time t_0 and F_{\max} is the maximal fluorescence achieved by the addition of buffer containing Triton X-100 (1%) that leads to the total release of SRB from LUVs.

2.7. Kinetic modeling of SRB release profiles

The SRB release kinetics from the various DPPC:CHOL formulations were subjected to mathematical models including zero-order, first-order, Higuchi, Hixson-Crowell, Korsmeyer-Peppas, Weibull and Baker-Lonsdale models. The model with the highest correlation coefficient R^2 was considered to be the best fit for the kinetic release (Boyapally et al., 2010).

Zero-order model. The zero-order model describes the system where the drug release rate is independent of its concentration (Hadjiioannou et al., 1993; Kalam et al., 2007). It can be represented by the equation:

$$Q_t - Q_0 = K_0 t \quad (2)$$

Where Q_t is the percentage of released SRB at time t (eq (1)), Q_0 is the percentage of released SRB at time t_0 and K_0 (slope of zero-order equation) is the zero-order release constant expressed in units of time^{-1} . Data obtained from in vitro SRB release was plotted versus time.

First-order model. According to the first-order model (Gibaldi and Feldman, 1967; Wagner, 1969), the release of the drug can be expressed by the equation:

$$\log C = \log C_0 - Kt/2.303 \quad (3)$$

Where C_0 is the initial concentration of drug, k is the first-order rate constant expressed in units of time^{-1} and t is the time. In our work, C represents the percentage of remaining SRB in vesicles at time t and C_0 is the total SRB released in the medium containing Triton X-100 (1%). The data obtained were plotted as log percentage of SRB remaining versus time. This yielded a straight line with a slope of $-K/2.303$.

Higuchi model. The Higuchi model is the first example of a mathematical model aimed to describe drug release from a matrix system (Higuchi, 1961). The model describes the release of drugs from an insoluble matrix as a square root of a time-dependent process based on Fickian diffusion. In our work, we used the simplified Higuchi model expressed by the following equation:

$$Q = K_H \times t^{1/2} \quad (\text{Higuchi, 1963}) \quad (4)$$

Where K_H (slope of Higuchi equation) is the Higuchi dissolution constant. The data obtained were plotted as percentage of released SRB versus square root of time.

Hixson-Crowell model. The Hixson-Crowell model describes the release from systems where there is a change in surface area and diameter of particles or tablets. The release is expressed by the equation:

$$Q_0^{1/3} - Q_t^{1/3} = \kappa_{hc} \times t \quad (\text{Hixson and Crowell, 1931}) \quad (5)$$

Where Q_t is the remaining amount of the drug in particles at time t , Q_0 is the initial amount of the drug and κ_{hc} , the obtained slope from the Hixson-Crowell calibration curve, is the release constant. In our work, $Q_0^{1/3}$ is the cube root of 100% percentage of total SRB released in the medium containing Triton X-100 and $Q_t^{1/3}$ represents the cube root of percentage of SRB remaining in liposomes at time t . This model was applied to evaluate if the release rate of SRB could be controlled by erosion, dissolution and degradation mechanisms. The data obtained were plotted as $(Q_0^{1/3} - Q_t^{1/3})$ versus time.

Baker-Lonsdale model. The Baker-Lonsdale (Baker and Lonsdale, 1974) described the drug release from a spherical matrix and expressed by the following equation:

$$\frac{3}{2} \left[1 - \left(1 - \frac{M_t}{M_\infty} \right)^{2/3} \right] \frac{M_t}{M_\infty} = Kt \quad (6)$$

This equation is used to linearize the release data from several formulations of microcapsules (Shukla and Price, 1991). The Taylor development of Baker-Lonsdale equation is outlined in the Supporting Information. Here, M_t/M_∞ is the percentage of released SRB at time t and K is the release rate constant obtained from the slope of Baker-Lonsdale equation $\sqrt{k}/2$. Data obtained from the in vitro SRB release from various batches of liposomes were plotted as $[d(M_t/M_\infty)]/dt$ with respect to the root of time inverse (Bhanja and Pal, 1989; Seki et al., 1990).

Weibull model. The Weibull model (Weibull, 1951) is used for drug dissolution or release from pharmaceutical dosage forms and expressed by the empirical equation: $m = 1 - e^{-(t - T/a)^b}$. In our work, m is the percentage of released SRB at time t , T accounts for the lag time before the onset of the dissolution or release process and in most cases will be zero, “ a ” denotes a scale parameter and is estimated from the calibration curve at time $t = 1$ (Kalam et al., 2007) while b is the shape parameter and obtained from the slope of the curve and characterizes the curve as exponential ($b = 1$), sigmoid ($b > 1$) or parabolic ($b < 1$). This empirical equation described above is rearranged as follows: $m = 1 - e^{-(t/a)^b}$ and its logarithmic form can be expressed by the equation:

$$\log [-\ln (1-m)] = b \log t - \log a \quad (7)$$

According to Weibull model, the dependency between the shape parameter b and the release mechanism has been established by several authors (Costa and Sousa Lobo, 2001). Fickian diffusion was estimated with $b \leq 0.75$, Fickian diffusion is combined with case II transport (matrix relaxation) with $0.75 < b < 1$ and a complex release mechanism of the drug is estimated with $b = 1$ (Papadopoulou et al., 2006). The data obtained were plotted as $\log [-\ln (1-m)]$ versus the log time.

Korsmeyer-Peppas model. The applicability of this model is restricted to the first 60% of drug release and expressed by the following equation:

$$M_t/M_\infty = Kt^n \quad (8)$$

Its logarithmic form could be written as $\log (M_t/M_\infty) = \log K + n \log t$.

Here, M_t/M_∞ corresponds to the first 60% of SRB released at time t , k is the release constant and n is release exponent. Data obtained were plotted as the log of 60% of released SRB with respect to the log time. The diffusional exponent n is obtained from the slope of Korsmeyer-Peppas equation and is indicative of the mechanism of release of SRB and is dependent on the geometry of the release device. The release exponent $n \leq 0.43$ indicates a diffusion-controlled drug release so-called Fickian diffusion; $0.43 < n < 1$ indicates a non-Fickian diffusion so-called anomalous transport in which the drug release is controlled by diffusion and erosion mechanisms; $n = 1$ indicates a zero-order release when the drug release is independent of time (Jafari and Kaffashi, 2016).

2.8. EPR spectroscopy measurements

2.8.1. Fluidity study

EPR spectra were carried out at various temperatures (293, 303, 313 and 323 K) on a Bruker 500E spectrometer at the X-band (9.4 GHz), equipped with Bruker N₂-temperature controller. The sample was introduced into a standard quartz EPR tube of 21 cm in length with an inner diameter of 3 mm and placed in EPR cavity for 2 min before the data acquisition to ensure thermal equilibration. EPR spectra were recorded using the following parameters: microwave power, 0.6–6.4 mW; modulation amplitude, 1 G; scan time, ~5 min; spectral resolution,

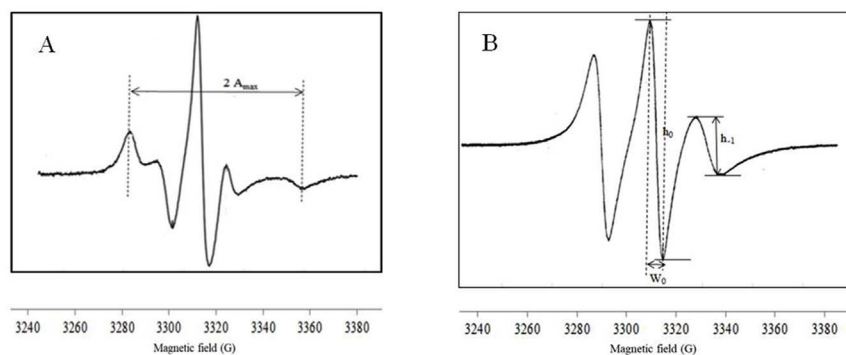


Fig. 1. EPR spectra of 5-DSA (A) and 16-DSA (B) labeled-DPPC liposomes.

2048 points; frequency modulation, 100 KHz.

The EPR spectrum of 5-DSA (Fig. 1A) exhibits anisotropic-low motion of the spin label. The fluidity of the membrane can be estimated from the outermost separation between the spectral extrema, the maximum hyperfine splitting ($2A_{\max}$). The value of $2A_{\max}$ reflects the motional profiles near the phospholipid polar head group of the lipid bilayer (Subongkot and Ngawhirunpat, 2015).

From 16-DSA spectrum (isotropic-fast motion) (Fig. 1B), the rotational correlation time (τ_c) is the liposomal fluidity parameter used to determine the motional profiles at the phospholipid acyl chain near the lipophilic region of the phospholipid bilayer (Subongkot and Ngawhirunpat, 2015). τ_c is calculated according to the formula (Keith et al., 1970):

$$\tau_c = (6.5 \times 10^{-10})W_0[(h_0/h_{-1})^{0.5} - 1] \quad (9)$$

Where W_0 is the width of the central peak in Gauss (G), h_0 and h_{-1} are the amplitude of the central and high field peaks respectively. The $2A_{\max}$ and τ_c increased with a decrease in fluidity (Sarrasague et al., 2012). EPR measurements were performed in triplicate for each labeled-DPPC:CHOL formulation.

2.9. Statistics

To assess significant differences between values, statistical analysis was carried out using the Student's t-test and the one-way analysis of variance (ANOVA). A value of $P < .05$ was considered statistically significant.

3. Results and discussion

3.1. Microscopy imaging of liposomes

TEM images showed a shape transition from irregular to nanosized unilamellar spherical vesicles following CHOL addition. Our findings are in agreement with a previous study proving that DPPC liposomes are subjected to shape fluctuation induced by CHOL addition (Brocca et al., 2004). The non-spherical shape was obtained for DPPC:CHOL formulations: 100:0 (Fig. 2A) and 100:2.5 (Fig. 2B). According to literature, the poor packing of lipid chains induces membrane defects (Raffy and Teissié, 1999) which in turn could be a reason for the irregular vesicle shape.

Beyond 2.5 mol% CHOL, liposomes were spherical, regular and homogenous in shape (Fig. 2C, D, E, F, G, H and I). According to literature, increasing CHOL content enhanced membrane stability (Nogueira et al., 2015) and this is associated with a decrease in membrane deformability due to an increase in lipid packing density (CHOL > 5%) (Choi et al., 2014).

3.2. Size and polydispersity index

The effect of CHOL addition on the mean size of DPPC liposomes

and PDI values was investigated by DLS and results were outlined in Table 1.

Table 1 showed a gradual increase in the mean size of DPPC vesicles from 220 to 472 nm following CHOL addition (< 30 mol%). However, further CHOL addition (50 and 100%) had a limited effect on the mean vesicles size and the values were about 400 nm. Insertion of CHOL inside the membrane leads to the formation of CHOL-poor and CHOL-rich domains that could coalesce into larger vesicles (López-Pinto et al., 2005; Tseng et al., 2007). The formation of raft domains at high CHOL content (50 and 100% CHOL) (Javanainen et al., 2017; Waheed et al., 2012) may result in no additional increase of the vesicle size. This latter can be also due to the fact that all formulations underwent extrusion through polycarbonate membrane of 0.4 μm . The liposome preparations were also characterized for their homogeneity and the obtained PDI values were in the range 0.40–0.42 (Table 1) suggesting a mono-dispersed population of liposomes.

3.3. Release kinetics of SRB from liposomes

Most of the membrane permeability studies have been carried out using LUVs (Faure et al., 2006). They are prepared by reverse phase evaporation technique and their aqueous cavity allows a high encapsulation of hydrophilic fluorescent dyes (Ding et al., 2005; Khreich et al., 2008). SRB and calcein are mostly used as fluorescent probes to monitor liposomes permeability (Chen et al., 2012; Ding et al., 2005). In this work, permeability study of DPPC liposomes that differ by their cholesterol content was investigated by monitoring the release kinetics of SRB at 37 °C over 48 h.

Fig. 3 represents the release kinetics of SRB from various DPPC:CHOL batches. All the formulations containing CHOL% equal or below 30%, and DPPC:CHOL 100:75 showed a biphasic pattern, while a monophasic pattern was obtained for formulations loaded with DPPC:CHOL 100:50 and 100:100. The monophasic pattern was maintained during 28 days of incubation at 37 °C for the formulation DPPC:CHOL 100:100 (data not shown) allowing total release of SRB.

CHOL-free DPPC liposomes showed a release of SRB from the first hour of incubation and the percentage of released SRB was $6.84 \pm 0.09\%$. Compared to this batch, liposomes incorporating 2.5% and 10% of CHOL showed also a release of SRB and the percentage of SRB release after 1 h was $7.9 \pm 1.1\%$ and $6.1 \pm 0.65\%$ respectively. After the same time, the percentage of released SRB did not exceed 5% for the other DPPC:CHOL formulations. After 4 h of incubation, the release of SRB was fast for the formulations 100:0 and 100:2.5 where the percentage of released SRB reached 26%. However, this percentage was $16.41 \pm 1.01\%$ for the batch prepared at a molar ratio DPPC:CHOL of 100:10 and lower than 10% for the other formulations.

After 10 h of incubation, the percentage of released SRB was above 45% for DPPC:CHOL formulations of 100:0, 100:2.5 and 100:10. However, it was of 17 and 14% for the batches 100:20 and 100:30 respectively and below 10% for the formulations 100:50 and 100:100. Chen et al. (2012) reported that about 43% of calcein release from

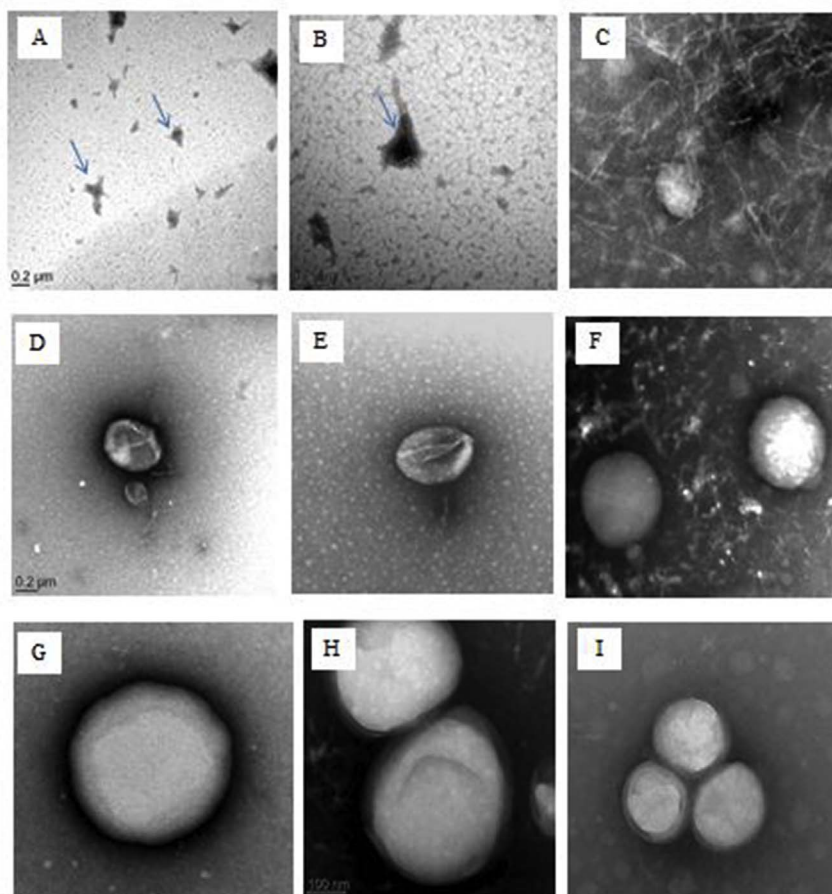


Fig. 2. TEM images of DPPC liposomes differing by their CHOL content: 0% (A), 2.5% (B), 5% (C), 10% (D), 20% (E), 25% (F), 30% (G), 50% (H) and 100% (I).

Table 1
Mean size values and polydispersity index for various DPPC:CHOL formulations.

| DPPC | CHOL | Size (nm) | PdI |
|------|------|------------|-------------|
| 100 | 0 | 220 ± 3.72 | 0.42 ± 0.31 |
| 100 | 2.5 | 221 ± 3.25 | 0.41 ± 0.07 |
| 100 | 5 | 278 ± 3.56 | 0.42 ± 0.30 |
| 100 | 10 | 300 ± 2.39 | 0.40 ± 0.09 |
| 100 | 20 | 308 ± 1.80 | 0.40 ± 0.07 |
| 100 | 25 | 467 ± 1.56 | 0.40 ± 0.04 |
| 100 | 30 | 472 ± 0.54 | 0.41 ± 0.39 |
| 100 | 50 | 400 ± 0.59 | 0.40 ± 0.07 |
| 100 | 100 | 402 ± 0.26 | 0.40 ± 0.10 |

Values are expressed as the means of three repetitions ± SD.

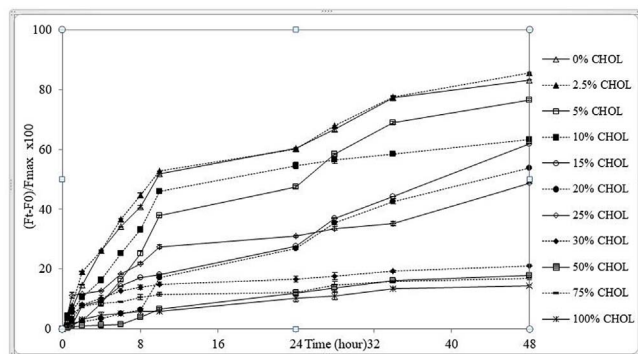


Fig. 3. The $(F_t - F_0)/F_{max} \times 100$ variation with time at 37 °C for DPPC:CHOL liposomes. Values are expressed as the mean of three independent release kinetics ± SD.

DPPC liposomes at 37 °C was obtained after 10 h of incubation (Chen et al., 2012). Similar results were obtained in our experiments since 45% of SRB were released after 10 h from CHOL-free DPPC liposomes.

After 48 h of incubation, the percentage of released SRB was higher than 80% for the formulations of 100:0 and 100:2.5, equals to 63, 53, 21%, for the formulations of 100:10, 100:20 and 100:30, and lower than 20% for the formulations of 100:50 and 100:100.

For formulations presenting a biphasic pattern of SRB release, the initial fast release could be due to SRB molecules adsorbed on the liposome surface, it is followed by a landing (between 10 and 24 h), then a re-increase of the SRB release. The second release phase may be attributed to the diffusion of SRB from the inner aqueous compartment to the extravascular medium. It seems that a landing period is required to allow a hydrophilic compound to cross the membrane.

McConnell and Radhakrishnan proposed that when cholesterol is added to the phospholipid membrane, the complex cholesterol-phospholipid is formed and the area of the membrane decreases until an equivalence point of 33 mol% of cholesterol is reached (McConnell and Radhakrishnan, 2003). Beyond 33 mol% of cholesterol, a little additional change was reported. Our results proved that the release of SRB was drastically decreased with the increase of the cholesterol content in DPPC:CHOL formulations up to 30%. Several works reported that an increase in cholesterol content in DPPC:CHOL systems produced a decrease in cross-sectional area per molecule (Mills et al., 2008; Ohvo-Rekila, 2002; Saito and Shinoda, 2011). This is translated by the “condensing effect” or “ordering effect” of cholesterol leading to a more rigid structure of the membrane (Cournia et al., 2007; Decker et al., 2012; Simons and Vaz, 2004).

The mechanical rigidity of liposomes induced by the condensing effect of cholesterol and defined as the bending stiffness (Takechi-Haraya et al., 2016) has been demonstrated using several methods. It

was demonstrated that the bending stiffness increased as a function of cholesterol for saturated phosphatidylcholine chains (Arriaga et al., 2009; Decker et al., 2012). Consequently, the increase of membrane rigidity induced by cholesterol seems to be accompanied with the decrease of lipid bilayer permeability.

According to literature, the DPPC lipid bilayer exists in a solid-ordered form described as the gel phase S_0 at low temperature (below 30 °C). DPPC bilayers undergo a gel-liquid crystal transition at 41.2 °C (T_m) where the lipid chains melt into a disordered-liquid structure L_d (Schubert et al., 2011; Tristram-Nagle and Nagle, 2004). Cholesterol affects the bilayer phase behavior (Feigenson, 2009; McMullen et al., 2004) and is considered as a key regulator of the membrane fluidity (Bagatolli and Sunil Kumar, 2009; Redondo-Morata et al., 2012; Xiang and Anderson, 1998). During the transition (S_0 to L_d phase), CHOL addition (< 30 mol%) leads to a gradual decrease in fluidity (Fraňová, 2010; Zhang et al., 2015), and this is accompanied by a decrease of SRB release for formulations (5 < CHOL% < 30). Also, at low CHOL content (2.5%), the SRB release kinetics were similar as that of the control. At this fraction, CHOL didn't affect the bilayer permeability which is also accompanied with the lower effect of CHOL on the lipid transition temperature (Waheed et al., 2012).

Above 30 mol% of cholesterol and at temperature ranging between 283 and 323 K, the lipid chains are tightly packed (Ohvo-Rekila, 2002), the membrane lipids adopted a liquid-ordered L_o phase (Aguilar et al., 2012; Saito and Shinoda, 2011) and cholesterol molecules arranged themselves in linear clusters (Zhang et al., 2015). Also, above CHOL 30%, minor changes of the liposome size, the bilayer thickness, and the average area per lipid molecule (Casciola et al., 2014; de Meyer and Smit, 2009) were observed and accompanied by a little variation of SRB release.

3.4. Mathematical modeling

To determine the effect of cholesterol on the constant release kinetics, quantitative analysis is done using the SRB release data. Several works applied mathematical models to evaluate the drug release mechanism from encapsulation systems (Shoab et al., 2010). Mathematical modeling can serve to optimize the design of therapeutic device based on the drug release kinetics results (Ait-Oudhia et al., 2014; Briuglia et al., 2015; Fugit and Anderson, 2014). Zero-order, first-order, Higuchi, Korsmeyer-Peppas, Hixson-Crowell, Weibull and Baker-Lonsdale models are the commonly used models describing the mechanism of drug release (Barzegar-Jalali et al., 2008; Costa and Sousa Lobo, 2001; Javadzadeh et al., 2010). The model that best fitted the release data was evaluated by the highest correlation coefficient R^2 (Costa and Sousa Lobo, 2001; Kadivar et al., 2015). The SRB release data were analyzed by the various mathematical models; the release constants values (K_1 and K_2) were determined for two period ranges (from 0 to 10 h and from 10 to 48 h, respectively). K_1 and K_2 values were summarized in Tables 2 and 3 respectively. A representative graph of each CHOL molar ratio with Korsmeyer-Peppas model (first and second release phases) is presented in the Supporting Information (Fig. s1).

Whatever the mathematical model used, the SRB release constants showed a decrease with the increase of CHOL content in the liposomal membrane. K_1 values decreased from 5.05 to 0.60 (zero order model), from 0.070 to 0.006 (first order model), from 16.87 to 2.24 (Higuchi model), from 0.97 to 0.73 (Weibull model), 0.09 to 0.009 (Hixson-Crowell model) and from 0.04 to 0.03 (Baker-Lonsdale model). Also for K_2 values, the variation was from 0.88 to 0.22 (zero order model), from 0.029 to 0.002 (first order model), from 8.80 to 2.14 (Higuchi model), from 0.95 to 0.54 (Weibull model), from 0.03 to 0.003 (Hixson-Crowell model), and from 0.04 to 0.03 (Baker-Lonsdale model).

In the first phase (0–10 h), data kinetics were fitted into the Weibull model. Results suggest a non-Fickian diffusion for formulations (CHOL

% 0, 2.5, 10, 15 and 50) as the “b” parameter values were between 0.75 and 1 (Table 2). Also, the “b” parameter of the formulations CHOL% of 30 and 100 were close to 0.75. This was in accordance with the results obtained by Korsmeyer-Peppas model as the “n” values were between 0.43 and 1 for the most formulations (Table 2).

For the second phase (from 10 to 48 h), the SRB release data suggested a Fickian diffusion mechanism for formulations (CHOL% 10, 30, 50, 75 and 100) as the “b” parameter values determined by Weibull model were below 0.75, which is concomitant with the obtained n values (< 0.43) from Korsmeyer-Peppas model (Table 3). Non-Fickian diffusion in the second phase was suggested for formulations CHOL% 0 and 2.5, and was confirmed by Korsmeyer-Peppas model while a zero order release mechanism seems to govern the SRB release from formulations CHOL% 5 and 15. Consequently, the period of incubation should be taken into consideration in release kinetics studies through lipid membranes.

3.5. Electron paramagnetic resonance study

EPR spectroscopy technique is used to monitor the molecular dynamics, mobility and conformational changes of the lipid bilayers (Sarrasague et al., 2012). In this work, changes in DPPC membrane fluidity following CHOL addition are monitored using 5- and 16-DSA as spin labels at the 5th and 16th carbon atom positions of the phospholipid acyl chain, respectively. The outer hyperfine splitting ($2A_{max}$) (Fig. 4A) and rotational correlation time (τ_c) (Fig. 4B) were the EPR parameters obtained from 5-DSA and 16-DSA spectra, respectively at various temperatures (293, 303, 313 and 323 K).

Free-CHOL liposomes showed a decrease in the EPR parameters with temperature where the $2A_{max}$ values decreased from 63.19 ± 0.37 to 57.41 ± 0.47 G and τ_c values decreased from 2.27 ± 0.37 to 1.26 ± 0.13 ns when temperature varied from 293 to 323 K. It is well-documented that DPPC vesicles undergo a transition from gel to liquid-crystalline state at the main transition temperature ($T_m \sim 314$ K) (Altunayar et al., 2015; Redondo-Morata et al., 2012) and a fluid phase appears above T_m . Since the maximum hyperfine splitting and rotational correlation time are inversely related to the fluidity (Coderch et al., 2000), a decrease in the $2A_{max}$ and τ_c parameters are observed for all DPPC:CHOL formulations with the raise of temperature which is in agreement with other studies. Compared to CHOL-free DPPC liposomes, and based on $2A_{max}$ values, the membrane fluidity increased ($P < .05$) for formulations 10 and 30% CHOL at 293 K; 20% CHOL at 303 K; 10% CHOL at 313 K and 20% CHOL at 323 K while it decreased ($P < .05$) for formulations with 20% CHOL at 313 K, 30% CHOL at 313 and 323 K and 100% CHOL at all the studied temperatures. This means that cholesterol, at low or intermediate percentage, increased the fluidity of the upper region of the membrane while it decreased it at high cholesterol content.

Also, compared to CHOL-free DPPC liposomes, the lipid membrane fluidity estimated by τ_c parameter at the hydrophobic end showed a decrease for formulations of 20, 30 and 100% CHOL at 293 K; 30 and 100% CHOL at 303 K; 10, 20, 30 and 100% CHOL at 313 and 323 K. The fluidity of deeper region of the membrane seems to be more affected by the cholesterol presence whatever was the CHOL content mainly above 313 K. Compared to CHOL-free DPPC membrane, the molecular dynamics near the hydrophobic region were not affected in formulations with 10% CHOL at 293 and 303 K.

On the overall, the membrane fluidity was not affected by low CHOL content (10%) in the hydrophobic core (16-DSA spectrum) while it was decreased near phospholipid head groups and inside the deep hydrophobic region at intermediate (20 and 30%) and high (100%) CHOL content and this is in agreement with other studies (Nagimo et al., 1991; Zhao et al., 2007). CHOL is located inside the lipid bilayer and not only near the polar head groups of phospholipids above CHOL 10%.

Table 2

Release rate constants of SRB (in the first phase, K1) and correlation coefficient values obtained for different DPPC:CHOL formulations using various mathematical models.

| Liposome formulation DPPC:CHOL | Zero-order K ± SD R ² ± SD | First-order K ± SD R ² ± SD | Higuchi K ± SD R ² ± SD | Korsmeyer-Peppas n ± SD R ² ± SD | Weibull b ± SD R ² ± SD | Hixson-Crowell K ± SD R ² ± SD | Baker-Lonsdale K ± SD R ² ± SD |
|-----------------------------------|---------------------------------------------|----------------------------------------------|------------------------------------------|---------------------------------------------------|------------------------------------------|-------------------------------------------------|-------------------------------------------------|
| 100:0 | 5.05 ± 0.00 0.9874 ± 0.02 | 0.070 ± 0.01 0.9937 ± 0.02 | 16.87 ± 0.00 0.9632 ± 0.01 | 0.87 ± 0.01 0.9944 ± 0.00 | 0.97 ± 0.00 0.9940 ± 0.00 | 0.97 ± 0.00 0.9972 ± 0.00 | 0.04 ± 0.00 0.4069 ± 0.04 |
| 100:2.5 | 5.16 ± 0.00 0.9779 ± 0.00 | 0.072 ± 0.03 0.9941 ± 0.00 | 17.41 ± 0.00 0.9726 ± 0.01 | 0.81 ± 0.00 0.9847 ± 0.02 | 0.91 ± 0.00 0.9728 ± 0.01 | 0.10 ± 0.00 0.9910 ± 0.01 | 0.07 ± 0.01 0.3467 ± 0.00 |
| 100:5 | 3.63 ± 0.01 0.9603 ± 0.01 | 0.043 ± 0.01 0.9340 ± 0.05 | 11.35 ± 0.00 0.8147 ± 0.01 | 1.23 ± 0.00 0.9768 ± 0.00 | 1.30 ± 0.00 0.9728 ± 0.01 | 0.06 ± 0.00 0.9437 ± 0.01 | 0.05 ± 0.00 0.6102 ± 0.03 |
| 100:10 | 4.24 ± 0.01 0.9893 ± 0.02 | 0.053 ± 0.00 0.9710 ± 0.00 | 13.54 ± 0.01 0.9148 ± 0.02 | 0.78 ± 0.02 0.9821 ± 0.05 | 0.85 ± 0.00 0.9723 ± 0.00 | 0.07 ± 0.00 0.9791 ± 0.01 | 0.03 ± 0.00 0.2254 ± 0.01 |
| 100:15 | 1.98 ± 0.02 0.9428 ± 0.01 | 0.021 ± 0.00 0.9517 ± 0.03 | 6.61 ± 0.003 0.9451 ± 0.00 | 1.19 ± 0.00 0.9201 ± 0.03 | 1.20 ± 0.04 0.9247 ± 0.00 | 0.032 ± 0.00 0.9489 ± 0.00 | 0.01 ± 0.00 0.1635 ± 0.00 |
| 100:20 | 1.31 ± 0.00 0.7979 ± 0.03 | 0.014 ± 0.00 0.7786 ± 0.02 | 4.03 ± 0.00 0.6623 ± 0.01 | 0.76 ± 0.00 0.8756 ± 0.00 | 0.74 ± 0.00 0.8673 ± 0.00 | 0.021 ± 0.00 0.7851 ± 0.00 | 0.01 ± 0.00 0.1004 ± 0.00 |
| 100:25 | 2.30 ± 0.00 0.9101 ± 0.01 | 0.025 ± 0.00 0.9255 ± 0.02 | 7.96 ± 0.00 0.9434 ± 0.00 | 0.56 ± 0.00 0.8693 ± 0.01 | 0.55 ± 0.00 0.8772 ± 0.00 | 0.037 ± 0.00 0.9207 ± 0.00 | 0.32 ± 0.00 0.4636 ± 0.00 |
| 100:30 | 1.41 ± 0.03 0.8835 ± 0.01 | 0.013 ± 0.00 0.8949 ± 0.01 | 5.20 ± 0.00 0.9659 ± 0.02 | 0.77 ± 0.00 0.9306 ± 0.01 | 0.72 ± 0.03 0.9346 ± 0.00 | 0.024 ± 0.00 0.8913 ± 0.00 | 0.23 ± 0.01 0.6832 ± 0.00 |
| 100:50 | 0.56 ± 0.00 0.8680 ± 0.01 | 0.005 ± 0.00 0.8631 ± 0.01 | 1.70 ± 0.00 0.7195 ± 0.00 | 0.96 ± 0.00 0.9066 ± 0.01 | 0.99 ± 0.00 0.9053 ± 0.01 | 0.008 ± 0.00 0.8649 ± 0.01 | 0.33 ± 0.00 0.1005 ± 0.04 |
| 100:75 | 0.95 ± 0.00 0.8103 ± 0.01 | 0.010 ± 0.00 0.9371 ± 0.02 | 3.57 ± 0.00 0.9547 ± 0.00 | 0.44 ± 0.01 0.9347 ± 0.02 | 0.45 ± 0.03 0.9364 ± 0.00 | 0.015 ± 0.00 0.8186 ± 0.00 | 0.20 ± 0.01 0.6228 ± 0.00 |
| 100:100 | 0.60 ± 0.01 0.8566 ± 0.00 | 0.006 ± 0.00 0.8604 ± 0.00 | 2.24 ± 0.00 0.8624 ± 0.01 | 0.79 ± 0.00 0.9244 ± 0.01 | 0.73 ± 0.00 0.9253 ± 0.01 | 0.009 ± 0.00 0.8592 ± 0.01 | 0.03 ± 0.00 0.2536 ± 0.01 |

The emergence of the raft-like domains in membranes (Javanainen et al., 2017; Topozini et al., 2014) at intermediate and high CHOL content may explain the decrease in membrane fluidity and consequently the permeability for SRB.

4. Conclusion

To sum up, in this work we focused on the understanding and modeling the bilayer permeability and fluidity of DPPC liposomes containing various CHOL percentages. Regular shapes of liposomes with a CHOL content higher than (2.5%) were obtained, and this was associated with a decrease in membrane deformability and a gradual decrease in the release of SRB. The SRB release data exhibited a

biphasic pattern for all formulations except those of CHOL% 50 and 100. A non-Fickian diffusion mechanism governs the SRB release in the first release phase for all formulations, and in the second phase for formulations CHOL% 0 and 2.5. However, a Fickian diffusion mechanism controls the SRB release after 10 h of incubation for formulations containing a percentage of CHOL above 5. The results of this study could be considered in lipid membrane permeability studies as well as in the development of delivery systems based on liposomes.

Conflicts of interest

The authors declare no conflict of interest.

Table 3

Release rate constants of SRB (in the second phase, K2) and correlation coefficient values obtained for different DPPC:CHOL formulations using various mathematical models.

| Liposome formulation DPPC:CHOL | Zero-order K ± SD R ² ± SD | First-order K ± SD R ² ± SD | Higuchi K ± SD R ² ± SD | Korsmeyer-Peppas n ± SD R ² ± SD | Weibull b ± SD R ² ± SD | Hixson-Crowell K ± SD R ² ± SD | Baker-Lonsdale K ± SD R ² ± SD |
|-----------------------------------|---------------------------------------------|----------------------------------------------|------------------------------------------|---------------------------------------------------|------------------------------------------|-------------------------------------------------|-------------------------------------------------|
| 100:0 | 0.88 ± 0.01 0.9430 ± 0.03 | 0.029 ± 0.00 0.9358 ± 0.00 | 8.80 ± 0.00 0.9293 ± 0.01 | 0.31 ± 0.00 0.9136 ± 0.00 | 0.95 ± 0.00 0.9496 ± 0.00 | 0.031 ± 0.00 0.9411 ± 0.01 | 0.023 ± 0.00 0.0105 ± 0.03 |
| 100:2.5 | 0.92 ± 0.01 0.9478 ± 0.02 | 0.032 ± 0.00 0.9342 ± 0.00 | 9.15 ± 0.00 0.9224 ± 0.01 | 0.31 ± 0.01 1.00 ± 0.00 | 1.05 ± 0.01 0.9727 ± 0.04 | 0.033 ± 0.00 0.9430 ± 0.00 | 0.05 ± 0.00 0.036 ± 0.01 |
| 100:5 | 1.09 ± 0.01 0.9355 ± 0.05 | 0.027 ± 0.00 0.9388 ± 0.00 | 10.88 ± 0.03 0.9248 ± 0.04 | 0.26 ± 0.00 1.00 ± 0.00 | 1.14 ± 0.00 0.9294 ± 0.00 | 0.031 ± 0.00 0.9404 ± 0.01 | 0.25 ± 0.00 0.3173 ± 0.01 |
| 100:10 | 0.45 ± 0.00 0.9632 ± 0.02 | 0.010 ± 0.00 0.9824 ± 0.01 | 4.62 ± 0.00 0.9932 ± 0.03 | 0.20 ± 0.00 0.9970 ± 0.01 | 0.34 ± 0.00 0.9908 ± 0.01 | 0.012 ± 0.00 0.9769 ± 0.00 | 0.23 ± 0.00 0.5399 ± 0.01 |
| 100:15 | 1.18 ± 0.00 0.9731 ± 0.01 | 0.020 ± 0.00 0.9432 ± 0.00 | 11.62 ± 0.00 0.9259 ± 0.00 | 0.68 ± 0.02 0.9282 ± 0.01 | 1.52 ± 0.00 0.9869 ± 0.01 | 0.026 ± 0.00 0.9556 ± 0.00 | 0.22 ± 0.00 0.4273 ± 0.01 |
| 100:20 | 1.00 ± 0.00 0.9740 ± 0.04 | 0.016 ± 0.00 0.9707 ± 0.05 | 9.96 ± 0.01 0.9530 ± 0.00 | 0.74 ± 0.01 0.9620 ± 0.03 | 1.25 ± 0.03 0.9641 ± 0.05 | 0.021 ± 0.00 0.9738 ± 0.00 | 0.28 ± 0.00 0.4691 ± 0.03 |
| 100:25 | 0.52 ± 0.01 0.8955 ± 0.01 | 0.009 ± 0.02 0.8672 ± 0.02 | 5.26 ± 0.01 0.8075 ± 0.02 | 0.32 ± 0.00 0.7738 ± 0.01 | 0.80 ± 0.01 0.9375 ± 0.00 | 0.012 ± 0.00 0.8767 ± 0.01 | 0.30 ± 0.01 0.4032 ± 0.00 |
| 100:30 | 0.17 ± 0.00 0.9739 ± 0.02 | 0.003 ± 0.00 0.9734 ± 0.00 | 1.65 ± 0.01 0.9421 ± 0.03 | 0.22 ± 0.01 0.9504 ± 0.00 | 0.40 ± 0.00 0.9881 ± 0.01 | 0.003 ± 0.00 0.9737 ± 0.01 | 0.32 ± 0.00 0.3470 ± 0.01 |
| 100:50 | 0.30 ± 0.02 0.8299 ± 0.01 | 0.003 ± 0.00 0.8687 ± 0.03 | 1.70 ± 0.01 0.8976 ± 0.02 | 0.68 ± 0.01 0.9393 ± 0.00 | 0.50 ± 0.02 0.6679 ± 0.03 | 0.005 ± 0.00 0.8336 ± 0.01 | 0.40 ± 0.00 0.1593 ± 0.02 |
| 100:75 | 0.15 ± 0.00 0.8581 ± 0.05 | 0.001 ± 0.00 0.8597 ± 0.06 | 1.52 ± 0.04 0.8027 ± 0.01 | 0.25 ± 0.00 0.8040 ± 0.00 | 0.45 ± 0.00 0.8084 ± 0.01 | 0.004 ± 0.00 0.8590 ± 0.01 | 0.21 ± 0.00 0.1562 ± 0.01 |
| 100:100 | 0.22 ± 0.00 0.9122 ± 0.04 | 0.002 ± 0.03 0.9159 ± 0.13 | 2.14 ± 0.01 0.9565 ± 0.02 | 0.58 ± 0.02 0.9742 ± 0.00 | 0.54 ± 0.02 0.8761 ± 0.00 | 0.003 ± 0.01 0.9147 ± 0.00 | 0.03 ± 0.00 0.1029 ± 0.01 |

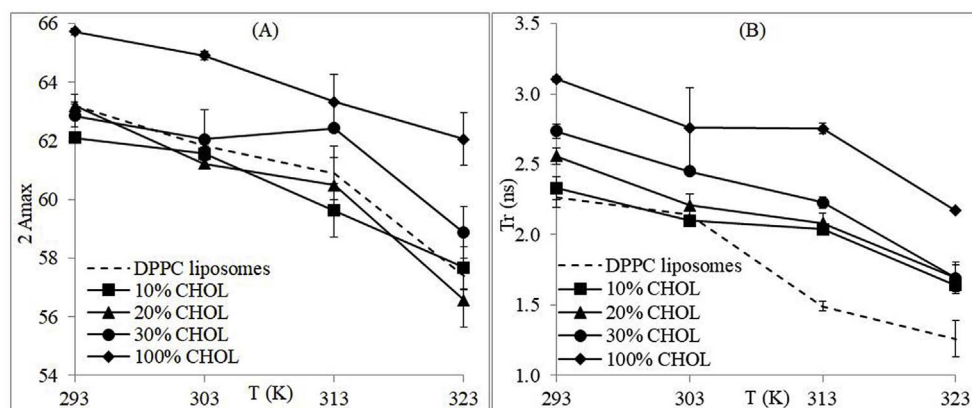


Fig. 4. Effect of temperature and CHOL content on EPR parameters: maximum hyperfine splitting (A) and rotational correlation time (B).

Acknowledgments

Authors thank the Agence Universitaire de la Francophonie (PCSI 2015–2017).

Appendix A. Supplementary data

Supplementary data related to this article can be found at <http://dx.doi.org/10.1016/j.fct.2018.01.017>.

Transparency document

Transparency document related to this article can be found online at <http://dx.doi.org/10.1016/j.fct.2018.01.017>.

References

- Aguilar, L.F., Pino, J. a., Soto-Arriaza, M. a., Cuevas, F.J., Sánchez, S., Sotomayor, C.P., 2012. Differential dynamic and structural behavior of lipid-cholesterol domains in model membranes. *PLoS One* 7 (6). <http://doi.org/10.1371/journal.pone.0040254>.
- Ait-Oudhia, S., Mager, D.E., Straubinger, R.M., 2014. Application of pharmacokinetic and pharmacodynamic analysis to the development of liposomal formulations for oncology. *Pharmaceutics* 6 (1), 137–174. <http://doi.org/10.3390/pharmaceutics6010137>.
- Akbarzadeh, A., Rezaei-Sadabady, R., Davaran, S., Joo, S.W., Zarghami, N., Hanifehpour, Y., Nejati-Koshki, K., 2013. Liposome: classification, preparation, and applications. *Nanoscale Research Letters* 8. Retrieved from: <http://www.ncbi.nlm.nih.gov/pubmed/23432972><http://www.pubmedcentral.nih.gov/articlerender.fcgi?artid=PMC3599573>.
- Altunayar, C., Sahin, I., Kazanci, N., 2015. A comparative study of the effects of cholesterol and desmosterol on zwitterionic DPPC model membranes. *Chem. Phys. Lipids* 188, 37–45. <http://doi.org/10.1016/j.chemphyslip.2015.03.006>.
- Arriaga, L.R., López-Montero, I., Monroy, F., Orts-Gil, G., Farago, B., Hellweg, T., 2009. Stiffening effect of cholesterol on disordered lipid phases: a combined neutron spin echo + dynamic light scattering analysis of the bending elasticity of large unilamellar vesicles. *Biophys. J.* 96 (9), 3629–3637. <http://doi.org/10.1016/j.bpj.2009.01.045>.
- Bagatolli, L., Sunil Kumar, P.B., 2009. Phase behavior of multicomponent membranes: experimental and computational techniques. *Soft Matter* 5 (17), 3234–3248. <http://doi.org/10.1039/B901866B>.
- Baker, R.W., Lonsdale, H.S., 1974. Controlled Release of Biologically Active Agents.
- Barzegar-Jalali, M., Adibkia, K., Valizadeh, H., Shadbad, M.R.S., Nokhodchi, A., Omid, Y., Shadbad, S., 2008. Kinetic analysis of drug release from nanoparticles. *J. Pharm. Pharmaceut. Sci.: A Publication of the Canadian Society for Pharmaceutical Sciences, Société Canadienne Des Sciences Pharmaceutiques* 11 (1), 167–177.
- Bhanja, R.S., Pal, T.K., 1989. In-vitro diffusion kinetics of salbutamol sulphate from microcapsules coated with Eudragit RS 100. *Boll. Chim. Farm.* 128 (9), 281–283. Retrieved from: <http://www.ncbi.nlm.nih.gov/pubmed/2635613>.
- Boyapally, H., Nukala, R.K., Bhujbal, P., Douroumis, D., 2010. Controlled release from directly compressible theophylline buccal tablets. *Coll. Surf. B Biointerf.* 77 (2), 227–233. <http://doi.org/10.1016/j.colsurfb.2010.01.031>.
- Bretscher, M., 1973. Membrane structure: some general principles. *Science* 181 (4100), 622–629. <http://doi.org/10.1126/science.181.4100.622>.
- Briuglia, M.L., Rotella, C., McFarlane, A., Lamprou, D.A., 2015. Influence of cholesterol on liposome stability and on in vitro drug release. *Drug Delivery and Translational Research* 5 (3), 231–242. <http://doi.org/10.1007/s13346-015-0220-8>.
- Brocca, P., Cantù, L., Corti, M., Del Favero, E., Motta, S., 2004. Shape fluctuations of large unilamellar lipid vesicles observed by laser light scattering: influence of the small-scale structure. *Langmuir* 20 (6), 2141–2148. <http://doi.org/10.1021/la035374v>.
- Bulbake, U., Doppalapudi, S., Kommineni, N., Khan, W., 2017. Liposomal formulations in clinical use: an updated review. *Pharmaceutics* 9 (2), 12. <http://doi.org/10.3390/pharmaceutics9020012>.
- Casciola, M., Bonhenry, D., Liberti, M., Apollonio, F., Tarek, M., 2014. A molecular dynamic study of cholesterol rich lipid membranes: comparison of electroporation protocols. *Bioelectrochemistry* 100, 11–17. <http://doi.org/10.1016/j.bioelechem.2014.03.009>.
- Chen, K.H., Mueannoom, W., Gaisford, S., Kett, V., 2012. Investigation into the effect of varying l-leucine concentration on the product characteristics of spray-dried liposome powders. *J. Pharm. Pharmacol.* 64 (10), 1412–1424. <http://doi.org/10.1111/j.2042-7158.2012.01521.x>.
- Choi, Y., Attwood, S.J., Hoopes, M.I., Drolle, E., Karttunen, M., Leonenko, Z., 2014. Melatonin directly interacts with cholesterol and alleviates cholesterol effects in dipalmitoylphosphatidylcholine monolayers. *Soft Matter* 10 (1), 206–213. <http://doi.org/10.1039/C3SM52064A>.
- Coderch, L., Fonollosa, J., De Pera, M., Estelrich, J., De La Maza, A., Parra, J.L., 2000. Influence of cholesterol on liposome fluidity by EPR. Relationship with percutaneous absorption. *J. Contr. Release* 68 (1), 85–95. [http://doi.org/10.1016/S0168-3659\(00\)00240-6](http://doi.org/10.1016/S0168-3659(00)00240-6).
- Costa, P., Sousa Lobo, J.M., 2001. Modeling and comparison of dissolution profiles. *Eur. J. Pharmaceut. Sci.* 13 (2), 123–133. [http://doi.org/10.1016/S0928-0987\(01\)00095-1](http://doi.org/10.1016/S0928-0987(01)00095-1).
- Cournia, Z., Ullmann, G.M., Smith, J.C., 2007. Differential effects of cholesterol, ergosterol and lanosterol on a dipalmitoyl phosphatidylcholine Membrane: A molecular dynamics simulation study. *J. Phys. Chem. B* 111 (7), 1786–1801. <http://doi.org/10.1021/jp065172i>.
- de Meyer, F., Smit, B., 2009. Effect of cholesterol on the structure of a phospholipid bilayer. *Proceedings of the National Academy of Sciences of the United States of America* 106 (10), 3654–3658. <http://doi.org/10.1073/pnas.0809959106>.
- Decker, C., Fahr, A., Kuntsche, J., May, S., 2012. Selective partitioning of cholesterol and a model drug into liposomes of varying size. *Chem. Phys. Lipids* 165 (5), 520–529. <http://doi.org/10.1016/j.chemphyslip.2012.04.001>.
- Ding, W.X., Qi, X.R., Li, P., Maitani, Y., Nagai, T., 2005. Cholesteryl hemisuccinate as a membrane stabilizer in dipalmitoylphosphatidylcholine liposomes containing saikosaponin-d. *Int. J. Pharm.* 300 (1–2), 38–47. <http://doi.org/10.1016/j.ijpharm.2005.05.005>.
- Eeman, M., Deleu, M., 2010. From biological membranes to biomimetic model membranes. *Biotechnol. Agron. Soc. Environ.* 14 (4), 719–736. Retrieved from: <http://popups.ulg.ac.be/Base/document.php?id=6568>.
- Faure, C., Nallet, F., Roux, D., Milner, S.T., Gauffre, F., Olea, D., Lambert, O., 2006. Modeling leakage kinetics from multilamellar vesicles for membrane permeability determination: application to glucose. *Biophys. J.* 91 (12), 4340–4349. <http://doi.org/10.1529/biophysj.106.088401>.
- Fraňová, J., 2010. Effects of DPH on DPPC–Cholesterol membranes with varying concentrations of cholesterol: from local perturbations to limitations in fluorescence anisotropy experiments. *J. Phys. Chem. B* 114 (8), 2704–2711. <http://doi.org/10.1021/jp908533x>.
- Feigenson, G.W., 2009. Phase diagrams and lipid domains in multicomponent lipid bilayer mixtures. *Biochim. Biophys. Acta Biomembr.* 1788 (1), 47–52. <http://doi.org/10.1016/j.bbmem.2008.08.014>.
- Fugit, K.D., Anderson, B.D., 2014. Dynamic, nonsink method for the simultaneous determination of drug permeability and binding coefficients in liposomes. *Mol. Pharm.* 11 (4), 1314–1325. <http://doi.org/10.1021/mp400765n>.
- Gibaldi, M., Feldman, S., 1967. Establishment of sink conditions in dissolution rate determinations. Theoretical considerations and application to nondisintegrating dosage forms. *J. Pharmaceut. Sci.* 56 (10), 1238–1242. <http://doi.org/10.1002/jps.2600561005>.
- Gmajner, D., Ulrigh, N.P., 2011. Thermotropic phase behaviour of mixed liposomes of archaeal diether and conventional diester lipids. *J. Therm. Anal. Calorim.* 106 (1), 255–260. <http://doi.org/10.1007/s10973-011-1596-4>.
- Gracià, R.S., Bezlyepkina, N., Knorr, R.L., Lipowsky, R., Dimova, R., 2010. Effect of cholesterol on the rigidity of saturated and unsaturated membranes: fluctuation and electrodeformation analysis of giant vesicles. *Soft Matter* 6 (7), 1472. <http://doi.org/10.1039/b920629a>.

- Hadjiioannou, T.P., Christian, G.D., Koupparis, M.A., Macheras, P.E., 1993. Quantitative Calculations in Pharmaceutical Practice and Research.
- Haeri, A., Alinaghian, B., Daeihamed, M., Dadashzadeh, S., 2014. Preparation and characterization of stable nanoliposomal formulation of fluoxetine as a potential adjuvant therapy for drug-resistant tumors. *Iran. J. Pharm. Res. (IJPR)* 13 (Suppl. L), 3–14.
- Higuchi, T., 1961. Rate of release of medicaments from ointment bases containing drugs in suspension. *J. Pharmaceut. Sci.* 50, 874–875. Retrieved from: <http://www.ncbi.nlm.nih.gov/pubmed/13907269>.
- Higuchi, T., 1963. Mechanism of sustained-action medication. Theoretical analysis of rate of release of solid drugs dispersed in solid matrices. *J. Pharmaceut. Sci.* 52 (12), 1145–1149. <http://doi.org/10.1002/jps.2600521210>.
- Hixson, A.W., Crowell, J.H., 1931. Dependence of reaction velocity upon surface and agitation. *Ind. Eng. Chem.* 23 (8), 923–931. <http://doi.org/10.1021/ie50260a018>.
- Jafari, M., Kaffashi, B., 2016. Mathematical kinetic modeling on isoniazid release from dex-HEMA-PNIPAAm nanogels. *Nanomed Res J* 1 (2), 90–96. <http://doi.org/10.7508/nmrj.2016.02.005>.
- Javadzadeh, Y., Ahadi, F., Davaran, S., Mohammadi, G., Sabzevari, A., Adibkia, K., 2010. Preparation and physicochemical characterization of naproxen-PLGA nanoparticles. *Colloids Surfaces B Biointerfaces* 81 (2), 498–502. <http://doi.org/10.1016/j.colsurfb.2010.07.047>.
- Javanainen, M., Martinez-Seara, H., Vattulainen, I., 2017. Nanoscale membrane domain formation driven by cholesterol. *Sci. Rep.* 7 (1), 1143. <http://doi.org/10.1038/s41598-017-01247-9>.
- Kadivar, A., Kamalidehghan, B., Javar, H.A., Davoudi, E.T., Zaharuddin, N.D., Sabeti, B., Noordin, M.I., et al., 2015. Formulation and in vitro, in vivo evaluation of effervescent floating sustained-release imatinib mesylate tablet. *PLoS One* 10 (6), 1–23. <http://doi.org/10.1371/journal.pone.0126874>.
- Kalam, M., Humayun, M., Parvez, N., Yadav, S., 2007. Release kinetics of modified pharmaceutical dosage forms: a review. *Cont. J. Pharmaceutical Sci.* 1 (January), 30–35. Retrieved from: <http://www.wiloludjournal.com/pdf/pharmsci/2007/30-35.pdf>.
- Keith, A., Bulfield, G., Snipes, W., 1970. Spin-labeled neurospora mitochondria. *Biophys. J.* 10 (7), 618–629. [http://doi.org/10.1016/S0006-3495\(70\)86324-X](http://doi.org/10.1016/S0006-3495(70)86324-X).
- Khreich, N., Lamourette, P., Boutal, H., Devilliers, K., Cr minon, C., Volland, H., 2008. Detection of Staphylococcus enterotoxin B using fluorescent immunoliposomes as label for immunochromatographic testing. *Anal. Biochem.* 377 (2), 182–188. <http://doi.org/10.1016/j.ab.2008.02.032>.
- L pez-Pinto, J.M., Gonz lez-Rodr guez, M.L., Rabasco, A.M., 2005. Effect of cholesterol and ethanol on dermal delivery from DPPC liposomes. *Int. J. Pharm.* 298 (1), 1–12. <http://doi.org/10.1016/j.ijpharm.2005.02.021>.
- Magarkar, A., Dhawan, V., Kallinteri, P., Viitala, T., Elmowafy, M., R g, T., Bunker, A., 2014. Cholesterol level affects surface charge of lipid membranes in saline solution. *Sci. Rep.* 4, 5005. <http://doi.org/10.1038/srep05005>.
- Masarudin, M.J., Cutts, S.M., Evison, B.J., Phillips, D.R., Pigram, P.J., 2015. Factors determining the stability, size distribution, and cellular accumulation of small, mono-disperse chitosan nanoparticles as candidate vectors for anticancer drug delivery: application to the passive encapsulation of [14C]-doxorubicin. *Nanotechnol. Sci. Appl.* 8, 67–80. <http://doi.org/10.2147/NSA.S91785>.
- McConnell, H.M., Radhakrishnan, A., 2003. Condensed complexes of cholesterol and phospholipids. *Biochim. Biophys. Acta Biomembr.* 1610 (2), 159–173. [http://doi.org/10.1016/S0005-2736\(03\)00015-4](http://doi.org/10.1016/S0005-2736(03)00015-4).
- McMullen, T.P.W., Lewis, R.N.A.H., McElhaney, R.N., 2004. Cholesterol-phospholipid interactions, the liquid-ordered phase and lipid rafts in model and biological membranes. *Curr. Opin. Colloid Interface Sci.* 8 (6), 459–468. <http://doi.org/10.1016/j.cocis.2004.01.007>.
- Miao, Z.L., Deng, Y.J., Du, H.Y., Suo, Bin, X., Wang, X.Y., Wang, X., Duan, N., 2015. Preparation of a liposomal delivery system and its in vitro release of rapamycin. *Experimental and Therapeutic Medicine* 9 (3), 941–946. <http://doi.org/10.3892/etm.2015.2201>.
- Mills, T.T., Toombes, G.E.S., Tristram-Nagle, S., Smilgies, D., Feigenson, G.W., Nagle, J.F., 2008. Order parameters and areas in fluid-phase oriented lipid membranes using wide angle x-ray scattering. *Biophys. J.* 95 (2), 669–681. <http://doi.org/10.1529/biophysj.107.127845>.
- Nagimo, A., Sato, Y., Suzuki, Y., 1991. Electron spin resonance studies of phosphatidylcholine interacted with cholesterol and with a hopanoid in liposomal membrane. *Chem. Pharmaceut. Bull.* 39 (11), 3071–3074. <http://doi.org/10.1248/cpb.39.3071>.
- Najafinobar, N., Mellander, L.J., Kurczy, M.E., Dunneval, J., Anger, T.B., Fletcher, J.S., Cans, A.-S., 2016. Cholesterol alters the dynamics of release in protein independent cell models for exocytosis. *Sci. Rep.* 6 (1), 33702. <http://doi.org/10.1038/srep33702>.
- Nogueira, E., Gomes, A.C., Preto, A., Cavaco-Paulo, A., 2015. Design of liposomal formulations for cell targeting. *Colloids Surfaces B Biointerfaces* 136, 514–526. <http://doi.org/10.1016/j.colsurfb.2015.09.034>.
- Ohvo-Rekila, H., 2002. Cholesterol interactions with phospholipids in membranes. *Prog. Lipid Res.* 41 (1), 66–97. [http://doi.org/10.1016/S0163-7827\(01\)00020-0](http://doi.org/10.1016/S0163-7827(01)00020-0).
- Papadopoulos, V., Kosmidis, K., Vlachou, M., Macheras, P., 2006. On the use of the Weibull function for the discernment of drug release mechanisms. *Int. J. Pharm.* 309 (1–2), 44–50. <http://doi.org/10.1016/j.ijpharm.2005.10.044>.
- Patil, Y.P., Jadhav, S., 2015. Preparation of liposomes for drug delivery applications by extrusion of giant unilamellar vesicles. In: *Nanoscale and Microscale Phenomena*, pp. 17–29. http://doi.org/10.1007/978-81-322-2289-7_2.
- Peetla, C., Vijayaraghavalu, S., Labhasetwar, V., 2013. Biophysics of cell membrane lipids in cancer drug resistance: implications for drug transport and drug delivery with nanoparticles. *Adv. Drug Deliv. Rev.* 65 (13–14), 1686–1698. <http://doi.org/10.1016/j.addr.2013.09.004>.
- Raffy, S., Teissie, J., 1999. Control of lipid membrane stability by cholesterol content. *Biophys. J.* 76 (4), 2072–2080. [http://doi.org/10.1016/S0006-3495\(99\)77363-7](http://doi.org/10.1016/S0006-3495(99)77363-7).
- Redondo-Morata, L., Giannotti, M.I., Sanz, F., 2012. Influence of cholesterol on the phase transition of lipid bilayers: a temperature-controlled force spectroscopy study. *Langmuir* 28 (35), 12851–12860. <http://doi.org/10.1021/la302620t>.
- Saito, H., Shinoda, W., 2011. Cholesterol effect on water permeability through DPPC and PSM lipid bilayers: a molecular dynamics study. *J. Phys. Chem. B* 115 (51), 15241–15250. <http://doi.org/10.1021/jp201611p>.
- Sarrasague, M., Cimato, A., Rubin de Celis, E., Facorro, G., 2012. Effect of serum proteins on an exogenous pulmonary surfactant: ESR analysis of structural changes and their relation with surfactant activity. *Respir. Physiol. Neurobiol.* 183 (1), 48–57. <http://doi.org/10.1016/j.resp.2012.05.023>.
- Schubert, T., Schneck, E., Tanaka, M., 2011. First order melting transitions of highly ordered dipalmitoyl phosphatidylcholine gel phase membranes in molecular dynamics simulations with atomistic detail. *J. Chem. Phys.* 135 (5), 1–11. <http://doi.org/10.1063/1.3615937>.
- Seki, T., Kawaguchi, T., Endoh, H., Ishikawa, K., Juni, K., Nakano, M., 1990. Controlled release of 3',5'-diester prodrugs of 5-Fluoro-2'-deoxyuridine from poly-L-lactic acid microspheres. *J. Pharmaceut. Sci.* 79 (11), 985–987. <http://doi.org/10.1002/jps.2600791108>.
- Sercombe, L., Veerati, T., Moheimani, F., Wu, S.Y., Sood, A.K., Hua, S., 2015. Advances and challenges of liposome assisted drug delivery. *Front. Pharmacol.* 6 (DEC), 1–13. <http://doi.org/10.3389/fphar.2015.00286>.
- Shoib, M.H., Al, S., Siddiqi, S., Yousuf, R.I., Zaheer, K., Hanif, M., Jabeen, S., 2010. Development and evaluation of hydrophilic colloid matrix of famotidine tablets. *AAPS PharmSciTech* 11 (2), 708–718. <http://doi.org/10.1208/s12249-010-9427-7>.
- Shukla, A.J., Price, J.C., 1991. Effect of drug loading and molecular weight of cellulose acetate propionate on the release characteristics of theophylline microspheres. *Pharmaceut. Res.* 8 (11), 1396–1400. <http://doi.org/10.1023/A:1015801207091>.
- Simons, K., Sampaio, J.L., 2011. Membrane organization and lipid rafts. *Perspect Biol* 3 (10), a004697. <http://doi.org/10.1101/cshperspect.a004697>.
- Simons, K., Vaz, W.L.C., 2004. Model systems, lipid rafts, and cell membranes. *Annu. Rev. Biophys. Biomol. Struct.* 33, 269–295. <http://doi.org/10.1146/annurev.biophys.32.110601.141803>.
- Subongkot, T., Ngawhirunpat, T., 2015. Effect of liposomal fluidity on skin permeation of sodium fluorescein entrapped in liposomes. *Int. J. Nanomed.* 10, 4581–4592. <http://doi.org/10.2147/IJN.S86624>.
- Tabandeh, H., Mortazavi, S.A., 2013. An investigation into some effective factors on encapsulation efficiency of alpha-tocopherol in MLVs and the release profile from the corresponding liposomal gel. *Iran. J. Pharm. Res. (IJPR)* 12 (Suppl. L), 19–28.
- Takechi-Haraya, Y., Sakai-Kato, K., Abe, Y., Kawanishi, T., Okuda, H., Goda, Y., 2016. Atomic force microscopic analysis of the effect of lipid composition on liposome membrane rigidity. *Langmuir* 32 (24), 6074–6082. <http://doi.org/10.1021/acs.langmuir.6b00741>.
- Toppozini, L., Meinhardt, S., Armstrong, C.L., Yamani, Z., Kucerka, N., Schmid, F., Rheinstadter, M.C., 2014. Structure of cholesterol in lipid rafts. *Phys. Rev. Lett.* 113 (22), 1–5. <http://doi.org/10.1103/PhysRevLett.113.228101>.
- Tristram-Nagle, S., Nagle, J.F., 2004. Lipid bilayers: thermodynamics, structure, fluctuations, and interactions. *Chem. Phys. Lipids* 127 (1), 3–14. <http://doi.org/10.1016/j.chemphyslip.2003.09.002>.
- Tseng, L.P., Liang, H.J., Chung, T.W., Huang, Y.Y., Liu, D.Z., 2007. Liposomes incorporated with cholesterol for drug release triggered by magnetic field. *J. Med. Biol. Eng.* 27 (1), 29–34.
- Wagner, J.G., 1969. Interpretation of percent dissolved-time plots derived from in vitro testing of conventional tablets and capsules. *J. Pharmaceut. Sci.* 58 (10), 1253–1257. <http://doi.org/10.1002/jps.2600581021>.
- Waheed, Q., Tj rnhammar, R., Edholm, O., 2012. Phase transitions in coarse-grained lipid bilayers containing cholesterol by molecular dynamics simulations. *Biophys. J.* 103 (10), 2125–2133. <http://doi.org/10.1016/j.bpj.2012.10.014>.
- Weibull, W., 1951. A statistical distribution function of wide applicability. *J. Appl. Mech.* 18, 293–297.
- Wu, C.H., Bialecka-Fornal, M., Newman, D.K., 2015. Methylation at the C-2 position of hopanoids increases rigidity in native bacterial membranes. *eLife* 4 (4), 1–18. <http://doi.org/10.7554/eLife.05663>.
- Xiang, T.X., Anderson, B.D., 1998. Influence of chain ordering on the selectivity of dipalmitoylphosphatidylcholine bilayer membranes for permeant size and shape. *Biophys. J.* 75 (6), 2658–2671. [http://doi.org/10.1016/S0006-3495\(98\)77111-2](http://doi.org/10.1016/S0006-3495(98)77111-2).
- Yang, J., Bahreman, A., Daudy, G., Bussmann, J., Olsthoorn, R.C.L., Kros, A., 2016. Drug delivery via cell membrane fusion using lipopeptide modified liposomes. *ACS Cent. Sci.* 2 (9), 621–630. <http://doi.org/10.1021/acscentsci.6b00172>.
- Zaske, A., Danila, D., Queen, M.C., Golunski, E., Conyers, J.L., 2013. Biological Atomic Force Microscopy for Imaging Gold-labeled Liposomes on Human Coronary Artery Endothelial Cells, 2013.
- Zhang, Y., Lervik, A., Seddon, J., Bresme, F., 2015. A coarse-grained molecular dynamics investigation of the phase behavior of DPPC/cholesterol mixtures. *Chem. Phys. Lipids* 185, 88–98. <http://doi.org/10.1016/j.chemphyslip.2014.07.011>.
- Zhao, L., Feng, S.S., Kocherginsky, N., Kostetski, I., 2007. DSC and EPR investigations on effects of cholesterol component on molecular interactions between paclitaxel and phospholipid within lipid bilayer membrane. *Int. J. Pharm.* 338 (1–2), 258–266. <http://doi.org/10.1016/j.ijpharm.2007.01.045>.